



Effect of dispersive optical phonons on the properties of the bond Su-Schrieffer-Heeger polaronChao Zhang ^{*}*Department of Modern Physics, University of Science and Technology of China, Hefei, Anhui 230026, China and Hefei National Laboratory, University of Science and Technology of China, Hefei, Anhui 230088, China* (Received 28 March 2023; revised 2 August 2023; accepted 7 August 2023; published 23 August 2023)

We use a newly developed quantum Monte Carlo method to investigate the impact of finite dispersion of the optical phonon mode on the properties of the bond Su-Schrieffer-Heeger polaron in two dimensions. We compare the properties of the bond polaron, such as effective mass, ground state energy, and Z factor, with and without positive phonon bandwidth. Our findings reveal that when we exclude phonon dispersion, at the same electron-phonon coupling strength, the effective mass increases as the phonon frequency decreases, indicating a heavier polaron in the deep adiabatic regime. However, in the dispersive case, we observe that the effective mass increases as the phonon bandwidth increases. Moreover, we notice a crossover from a light polaron state to a heavy polaron state in the deep adiabatic regime for both the dispersionless and dispersive cases.

DOI: [10.1103/PhysRevB.108.075156](https://doi.org/10.1103/PhysRevB.108.075156)**I. INTRODUCTION**

The polaron problem continues to draw significant attention in condensed matter physics. It studies the behavior of a particle when coupled to its environment. Depending on the characteristics of the particle, the environment, and their coupling, various types of polarons can arise, including polarons with electron-phonon interaction [1–7], spin polarons [8–10], Fermi polarons [11–14], and protons in neutron-rich matter [15]. Of particular significance is the polaron with electron-phonon interaction, as it plays a crucial role in understanding the mechanism of high-temperature superconductivity in the dilute-density regime. In the low-density limit, the electron-phonon interaction can bind two polarons together to form a single bipolaron, forming of a Bose-Einstein-condensate-like superconductor. However, for such a superconducting state to manifest, it is essential to have a bipolaron with a light effective mass and a robust phonon-mediated pairing potential.

Previous studies have demonstrated that in the Holstein model, where the electron-phonon coupling influences the electron density, both the effective mass of the polaron and the effective mass of the bipolaron exhibit an exponential increase under strong electron-phonon coupling strengths [16–19]. However, when the electron-phonon coupling affects the electron hopping, as seen in the bond Su-Schrieffer-Heeger (SSH) polaron, the situation takes a different turn [20,21]. Recently, there has been a notable surge in interest in studying bond SSH polarons and bipolarons, particularly when phonon dispersion is absent. In such cases, the effective mass is not exponentially large even at strong coupling regimes, resulting in the formation of light polarons [17,22,23]. Remarkably, when two polarons form a bound state, the resulting bipolaron maintains a sufficiently low effective mass [17], and its size remains small, indicating the potential for high-temperature

superconductivity [24,25]. It is important to note that in all of the mentioned cases, only phonons with the Einstein mode are considered. Extending the bond SSH model to include dispersion among localized (Einstein) phonons opens up new possibilities for investigation. However, such an extension presents challenges due to the scarcity of numerical techniques suitable for analyzing polaron and bipolaron models with dispersive phonons, even in the well-known Holstein model. As a result, there have been limited attempts in the literature to study such systems with dispersive phonons [26,27].

In the dilute density limit, in the Holstein model, the phonon degrees of freedom dress the electrons, giving rise to polaron and bipolaron formation. Previous studies [28,29] have investigated the influence of the dispersion among optical phonons on the polaron's effective mass in one dimension. However, Ref. [28] is limited to one dimension which is not physical, and the adiabatic regime $\omega_0/t < 1$ has not been explored due to this being computationally hard. At higher densities, the phonons mediate collective superconducting and charge-density-wave phases. A recent study employing the quantum Monte Carlo technique has demonstrated the significant influence of phonon dispersion on the formation of charge-density-wave order in a system with finite electron density [30]. However, the specific impact of finite dispersion of the optical phonon mode on the properties of the bond SSH model, particularly with regard to the effective mass, remains unexplored.

In this paper, we utilize a newly developed quantum Monte Carlo method to explore the influence of finite dispersion in the optical phonon mode on the properties of the bond SSH polaron in two dimensions. Our methodology combines the path-integral formulation for the particle sector with real-space diagrammatic techniques for the phonon sector [31]. Due to the “sign” problem associated with negative phonon bandwidth in this approach, we focus solely on the positive phonon bandwidth. Our study quantitatively investigates the properties of the bond polaron with dispersive phonons in two dimensions, encompassing phonon bandwidths W smaller

^{*} zhangchao1986sdu@gmail.com

than, equal to, and larger than the phonon frequency ω_0 . Additionally, we explore properties in the adiabatic regime down to $\omega_0/t = 0.3$. The rest of the paper is organized as follows. In Sec. II, we present the Hamiltonian of the bond SSH polaron. In Sec. III, we introduce how to extract the properties from the Green's function. In Sec. IV, we discuss the results, and Sec. V concludes the paper.

II. HAMILTONIAN

We consider a bond SSH electron-phonon coupling on a simple two-dimensional square lattice. In this model, the electronic hopping between two sites is modulated by a single oscillator centered on the bond connecting the two sites. The model is described by the Hamiltonian [32–35]

$$H_1 = -t \sum_{\langle i,j \rangle, \sigma} (c_{j,\sigma}^\dagger c_{i,\sigma} + \text{H.c.}) + \omega_0 \sum_{\langle i,j \rangle} \left(b_{i,j}^\dagger b_{i,j} + \frac{1}{2} \right) + g \sum_{\langle i,j \rangle, \sigma} (c_{j,\sigma}^\dagger c_{i,\sigma} + \text{H.c.}) (b_{i,j}^\dagger + b_{i,j}), \quad (1)$$

where $\langle i, j \rangle$ denotes the nearest-neighbor sites. b_i is the optical phonon annihilation operator on site i , $c_{i,\sigma}$ is the annihilation operator for the electron on site i with spin $\sigma \in \{\uparrow, \downarrow\}$, t is the electron hopping amplitude between the nearest-neighbor sites (we use it as the unit of energy), and g is the strength of the electron-phonon coupling of the hopping-displacement type. ω_0 is the local phonon frequency.

We generalize Eq. (1) to $H = H_1 + H_2$, to include a coupling strength t_{ph} between nearest-neighbor bonds for the phonons, with

$$H_2 = -t_{ph} \sum_{\langle\langle i,j \rangle\rangle, \langle\langle i',j' \rangle\rangle} (b_{i,j}^\dagger b_{i',j'} + \text{H.c.}). \quad (2)$$

Here, $\langle\langle i, j \rangle\rangle, \langle\langle i', j' \rangle\rangle$ denotes nearest-neighbor bonds. t_{ph} is the hopping amplitude for phonons between nearest-neighbor bonds, and it can be positive or negative. The sign of the phonon propagator changes when the phonon hopping amplitude $t_{ph} < 0$, causing the sign problem. So here, we only consider $t_{ph} > 0$. The inclusion of the nearest-neighbor hopping of the phonons $t_{ph} > 0$ leads to a finite phonon bandwidth $W = 8t_{ph}$. When considering the dispersive case, some of the phonons are softer, and the phonon frequency is lowered to $\omega_L = \omega_0 - W/2$.

The properties of the bond SSH polaron are controlled by two dimensionless parameters: (i) the effective coupling

$$\lambda = \frac{g^2}{2t\omega}, \quad (3)$$

where ω is defined as $\omega = \omega_0$ (with ω_0 being the local phonon frequency) for the dispersionless case and $\omega = \omega_L$ for the dispersive case; and (ii) the adiabaticity ratio ω_0/t . In this paper, we work in the adiabatic regime $\omega_0/t \leq 1.0$, where the phonon degree of freedom is considered to be comparable to or slower than the electron motion.

III. GREEN'S FUNCTION

In the following, we study the effect of the positive phonon bandwidth W at a certain phonon frequency ω_0 on the

properties of the bond polaron: the ground state energy, the effective mass, and the Z factor. The polaron energy $E(\mathbf{k})$ and $Z(\mathbf{k})$ factor at momentum \mathbf{k} can be extracted from the Green's function dependence on imaginary time τ . In the asymptotic limit $\tau \rightarrow \infty$, this dependence is governed by the ground state in the corresponding momentum sector, as follows from the spectral Lehmann representation. For the stable (nondecaying) quasiparticle state, we have

$$G(\mathbf{k}, \tau \rightarrow \infty) \rightarrow Z(\mathbf{k}) e^{-[E(\mathbf{k}) - \mu]\tau}. \quad (4)$$

The Z factor $Z(\mathbf{k}) = |\langle \mathbf{k} | \tilde{\mathbf{k}} \rangle|^2$ is given by the overlap between the polaron eigenstate $|\tilde{\mathbf{k}}\rangle$ and the free-electron state $|\mathbf{k}\rangle = c_{\mathbf{k}}^\dagger |0\rangle$. The effective polaron mass is obtained from $m^*/m_0 = 2t / \frac{\partial^2 E(\mathbf{k})}{\partial \mathbf{k}^2}$, where the bare electron mass is $m_0 = 1/2a^2t$, with the lattice spacing $a = 1$. The chemical potential μ here is added to shift energies and control the rate of the exponential decays. It is used for computational convenience.

The newly developed quantum Monte Carlo method based on the path-integral formulation of the particle sector in combination with the real-space diagrammatic approach of the phonon sector is used here to study the effects of a finite dispersion of the optical phonon mode on the properties of the bond polaron [31], especially the effective mass. We explore a large adiabatic regime with ω_0/t as low as 0.3 and phonon bandwidth as large as $W = 1.5\omega_0$.

IV. RESULTS AND DISCUSSION

In this section, a comprehensive study of the bond polaron's properties as a function of electron-phonon coupling g/t for different phonon frequencies ω_0/t in the deep adiabatic regime and different phonon bandwidths W/t (smaller than, equal to, and larger than the phonon frequency) is provided. Although the properties of the bond polaron at $\omega_0/t = 0.5$ were investigated in Ref. [22] using the diagrammatic Monte Carlo method in the momentum space, we also put the results here for self-consistency and to set the stage for the discussion of the results with positive phonon bandwidth. We verify the correctness of our results by recalculating the phonon properties at $\omega_0/t = 0.5$ using the newly developed quantum Monte Carlo method [31].

Dispersionless case. Figure 1 illustrates the main findings of our study for the dispersionless bond polaron in the deep adiabatic regime. We present the ground state energy E_{GS} [Fig. 1(a)], the effective mass m^*/m_0 [Fig. 1(b)], and the Z factor [Fig. 1(c)] as functions of the electron-phonon coupling g/t , while considering different phonon frequencies, for $\omega_0/t = 1.0, 0.75, 0.5, 0.375, 0.3, 0.25$, and 0.2 . The $E_{GS}(g/t)$ curves for all phonon frequencies demonstrate a smooth evolution of the ground state energy with increasing g/t . Remarkably, the ground state energy decreases rapidly as the system enters the deep adiabatic regime. Regarding the effective mass, we observe a consistent increase as the phonon frequency decreases, for a fixed electron-phonon coupling g/t . Specifically, at $\omega_0/t = 1.0$, the effective mass exhibits a linear growth at weak and medium coupling strengths ($g/t \sim 2.0$) before experiencing a change in slope. This trend becomes more pronounced with decreasing ω_0/t . When $\omega_0/t = 0.2$, the effective mass shows a linear increase until the coupling strength reaches around $g/t \approx 0.4$, beyond which it

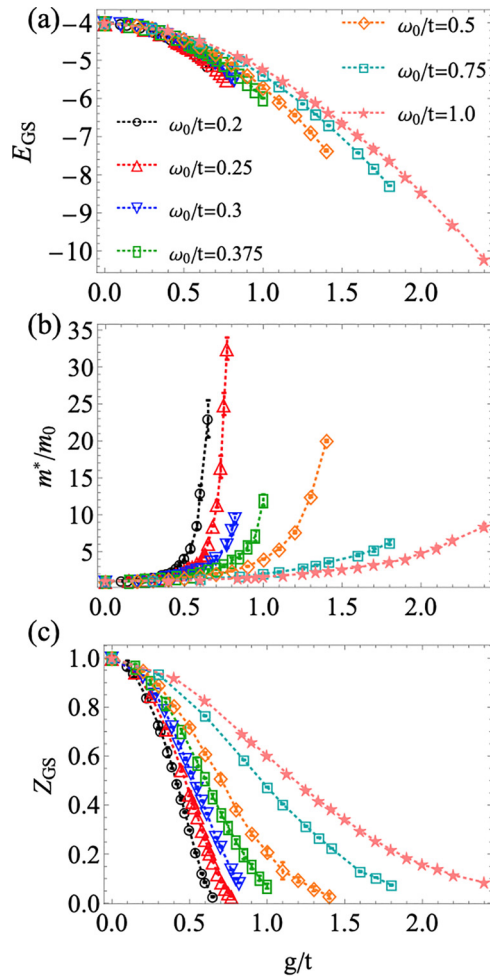


FIG. 1. The properties of the bond polaron: ground state energy E_{GS} (a), effective mass m^*/m_0 (b), and Z factor (c) as a function of electron-phonon coupling g/t for dispersionless phonon frequency $\omega_0/t = 0.2$ (black circles), 0.25 (red upward-pointing triangles), 0.3 (blue downward-pointing triangles), 0.375 (green rectangles), 0.5 (orange diamonds), 0.75 (cyan squares), and 1.0 (pink stars). If not visible, error bars are within the symbol size.

grows exponentially. This behavior signifies the existence of a crossover, wherein the polaron undergoes a change from a light state to a heavy state in the deep adiabatic regime, as discussed in detail later. Furthermore, the quasiparticle residue Z exhibits a smooth decrease as a function of g/t , with a rapid drop observed for smaller ω_0/t . Consequently, lowering the phonon frequency ω_0/t leads to a significantly heavier polaron at lower coupling strengths g/t .

Dispersive case. Figure 2 shows the ground state energy E_{GS} [Fig. 2(a)], the effective mass [Fig. 2(b)], and the Z factor [Fig. 2(c)] for phonon bandwidth $W/t = 0.5, 1.0,$ and 1.5 (representing bandwidths smaller than, equal to, and larger than the phonon frequency) in the adiabatic regime $\omega_0/t = 1.0$. In comparison to the dispersionless case with a phonon frequency of $\omega_0/t = 1.0$, the ground state energy E_{GS} decreases smoothly as the coupling strength increases, for all three bandwidths. Additionally, at the same electron-phonon coupling strength, the ground state energy is lower for a larger phonon bandwidth.

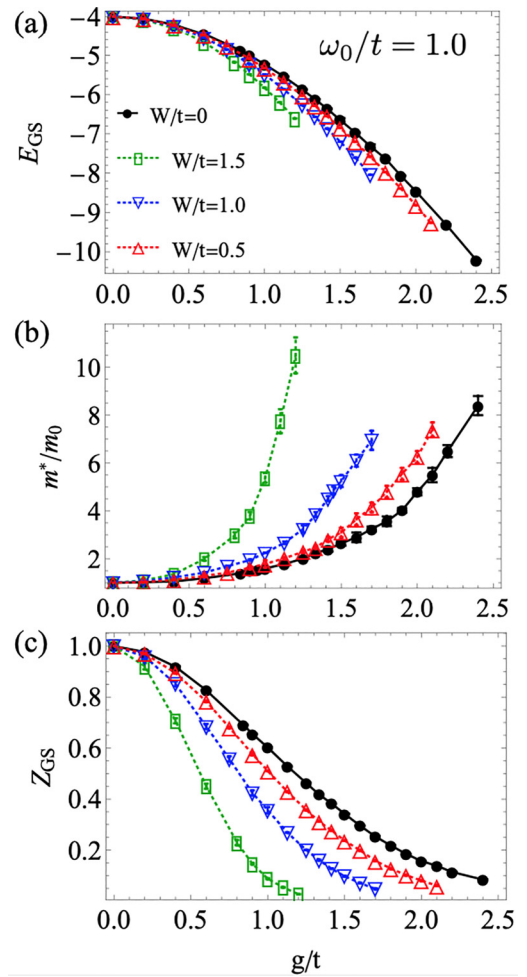


FIG. 2. The properties of the bond polaron with dispersive phonons: ground state energy E_{GS} (a), effective mass m^*/m_0 (b), and Z factor (c) as a function of the coupling strength g/t for dispersionless phonon frequency $\omega_0/t = 1.0$ (black circles) and the dispersive case with $\omega_0/t = 1.0$ and phonon bandwidth $W/t = 0.5$ (red upward-pointing triangles), $W/t = 1.0$ (blue downward-pointing triangles), and $W/t = 1.5$ (green rectangles). If not visible, error bars are within the symbol size.

The effective mass m^*/m_0 increases as a function of coupling strength g/t and changes its slope for larger coupling strength for all three phonon bandwidths W/t . However, due to the phonon dispersion, the phonon frequency is lowered as $\omega_L = \omega_0 - W/2$. For instance, when comparing the phonon bandwidth $W/t = 1.5$, the phonon frequency is lowered to $\omega_L/t = 0.25$. At a coupling strength of around $g/t \sim 0.75$, the effective mass m^*/m_0 is approximately 2.6. In contrast, for the dispersionless case $\omega_0/t = 0.25$ [red upward-pointing triangles in Fig. 1(b)], the effective mass increases exponentially around $g/t \sim 0.6$ and is approximately 26.0 for $g/t \sim 0.75$. Compared with the dispersionless case, the effective mass with dispersive phonons is lighter. When comparing with the lower frequency $\omega_0 = \omega_L$, with the positive phonon dispersion we tend to have a light polaron at strong coupling strength. The effective mass increases linearly at a weak coupling strength and becomes exponential at a strong coupling strength for a large phonon bandwidth $W/t = 1.5$. This

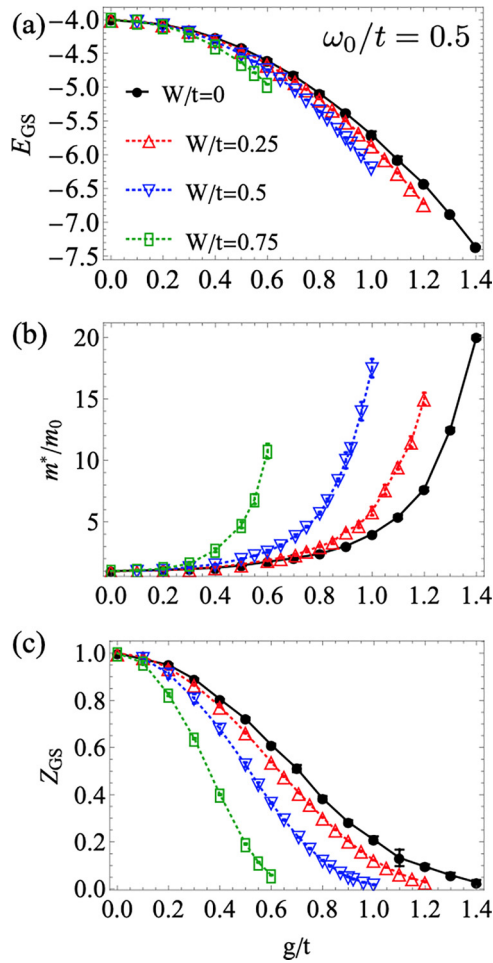


FIG. 3. The properties of the bond polaron with dispersive phonons: ground state energy E_{GS} (a), effective mass m^*/m_0 (b), and Z factor (c) as a function of the coupling strength g/t for dispersionless phonon frequency $\omega_0/t = 0.5$ (black circles) and the dispersive case with $\omega_0/t = 0.5$ and phonon bandwidth $W/t = 0.25$ (red upward-pointing triangles), $W/t = 0.5$ (blue downward-pointing triangles), and $W/t = 0.75$ (green rectangles). If not visible, error bars are within the symbol size.

indicates that there exists a crossover from a light polaron state to a heavy polaron state (see the discussion later).

The quasiparticle residue decreases smoothly as a function of g/t for all three bandwidths. At the same electron-phonon coupling g/t , the Z factor drops rapidly to zero as the bandwidth W/t increases.

The trend of the polaron properties is the same as the system goes into the deep adiabatic regime $\omega_0/t = 0.5$ for phonon bandwidth $W/t = 0.25, 0.5$, and 0.75 (shown in Fig. 3) and $\omega_0/t = 0.3$ for phonon bandwidth $W/t = 0.125, 0.25$, and 0.5 (shown in Fig. 4). However, the change in the effective mass becomes more abrupt. For instance, at $\omega_0/t = 0.5$ with bandwidth $W/t = 0.5$, the phonon frequency is lowered to $\omega_L/t = 0.25$, and the effective mass starts to increase exponentially around $g/t = 0.5$. When compared with the dispersionless case with $\omega_0/t = 0.25$ [red upward-pointing triangles in Fig. 1(b)], where the exponential growth of the effective mass starts around $g/t \sim 0.6$ and reaches

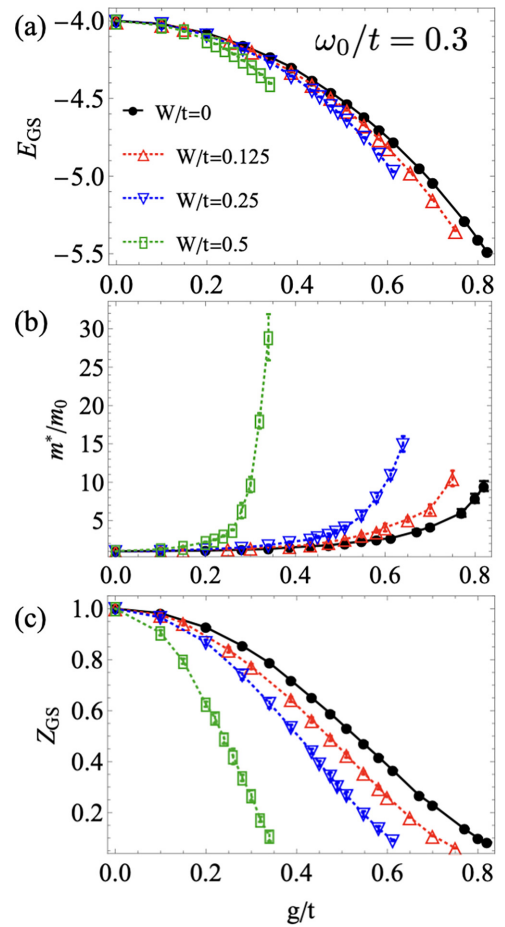


FIG. 4. The properties of the bond polaron with dispersive phonons: ground state energy E_{GS} (a), effective mass m^*/m_0 (b), and Z factor (c) as a function of the coupling strength g/t for dispersionless phonon frequency $\omega_0/t = 0.3$ (black circles) and the dispersive case with $\omega_0/t = 0.3$ and phonon bandwidth $W/t = 0.125$ (red upward-pointing triangles), $W/t = 0.25$ (blue downward-pointing triangles), and $W/t = 0.5$ (green rectangles). If not visible, error bars are within the symbol size.

$m^*/m_0 \sim 26.0$ at $g/t \sim 0.75$, the effective mass is around 4.6 at $g/t \sim 0.75$ in the dispersion case. Thus the polaron in the dispersive case is much lighter.

Similarly, for $\omega_0/t = 0.3$ with bandwidth $W/t = 0.25$, the phonon frequency is lowered to $\omega_L/t = 0.05$. The effective mass starts to increase exponentially around $g/t \sim 0.22$. Although we cannot obtain the exact value of the effective mass for $\omega_0/t = 0.05$ in the dispersionless case due to numerical challenges, it should be much heavier compared with the dispersive case, based on the trends shown in Fig. 1(b). Furthermore, at the same phonon frequency ω_0/t and electron-phonon coupling strength g/t , the effective mass increases more rapidly as the bandwidth increases. This observation can be explained by the fact that in the dispersive case, phonons are more mobile, leading to a more extended phonon cloud. Consequently, this extended phonon cloud effectively increases the effective mass of the electron by creating more obstacles for it to overcome as it moves through the lattice.

Overall, the results from $\omega_0/t = 1.0, 0.5$, and 0.3 in the presence of dispersive phonons suggest the formation of

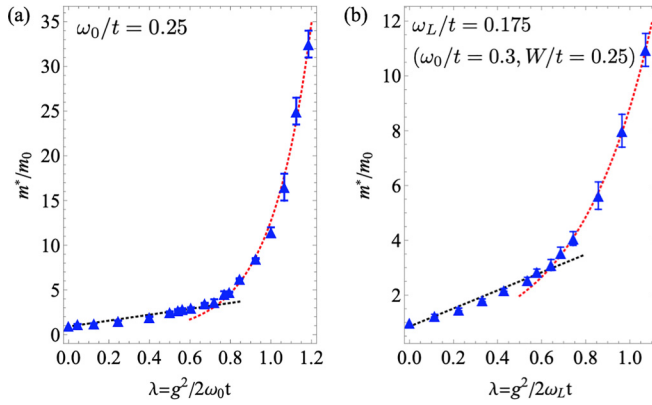


FIG. 5. (a) The effective mass m^*/m_0 as a function of the effective coupling $\lambda = g^2/2\omega_0 t$ at $\omega_0/t = 0.25$. (b) The effective mass as a function of the effective coupling $\lambda = g^2/2\omega_L t$ at $\omega_0/t = 0.3$ and phonon bandwidth $W/t = 0.25$. The black dotted line is a linear fit, and the red dotted line is an exponential fit for the effective mass as a function of effective coupling λ . There exists a crossover from a light bond polaron to an exponentially increasing heavy polaron as the electron-phonon coupling g/t increases.

relatively lighter polarons compared with the dispersionless case with the phonon frequency $\omega_0 = \omega_L$.

As previously mentioned, a crossover from a light polaron state to a heavy polaron state in the deep adiabatic regime occurs for both the dispersionless and dispersive cases. We further investigate the nature of this crossover in Fig. 5, where we study the effective mass as a function of the effective coupling λ for the dispersionless case with $\omega_0/t = 0.25$ [Fig. 5(a)] and the dispersive case with $\omega_0/t = 0.3$ [Fig. 5(b)] and phonon bandwidth $W/t = 0.25$. In the dispersive case, the phonon frequency is lowered to $\omega_L/t = 0.175$. In Fig. 5, the black dotted line represents a linear fit, and the red dotted line represents an exponential fit for the effective mass as a function of the effective coupling λ defined in Eq. (3). We observe that there exists a crossover from a light polaron state to a heavy polaron state with an exponential increasing of effective mass at $\lambda \sim 0.75$ for the dispersionless case with $\omega_0/t = 0.25$ and at $\lambda \sim 0.62$ for the dispersive case with $\omega_L/t = 0.175$. The crossover is characterized by an abrupt change in slope of the effective mass, showing a significant difference in the polaron's nature at the critical effective coupling in the deep adiabatic regime in both the dispersionless and dispersive cases.

V. CONCLUSION

We employed a recently developed quantum Monte Carlo method, which combines the path-integral formulation of the particle sector with the real-space diagrammatic approach of the phonon sector, to investigate the effects of finite dispersion in the optical phonon mode on the properties of the bond polaron. Our analysis focused on the ground state energy, effective mass, and Z factor of the bond polaron, considering different phonon frequencies as low as $\omega_0/t = 0.3$, corresponding to the deeply adiabatic regime, as well as the impact of positive phonon bandwidth on the bond polaron's properties.

Our findings revealed that, in the absence of dispersion, the effective mass increases as the phonon frequency decreases while keeping the electron-phonon coupling constant. In comparison, the dispersive case exhibited lighter effective masses, particularly at strong electron-phonon coupling strengths.

Moreover, our investigations demonstrated a crossover from a linear increase in effective mass to an exponential increase in effective mass in the deeply adiabatic regime, for both the dispersionless and dispersive cases. Notably, the dispersive case showed a lighter effective mass at strong coupling, suggesting the possibility of achieving a compact and light bipolaron in the strong coupling limit, potentially leading to an increase in the critical temperature T_c for the bond model. Achieving the higher T_c in the bond SSH model requires that the relative materials be in the same parameter regime as described in Refs. [24,25], which means (i) the interference of tunneling pathways should be controlled by light atoms, for example, hydrogen with large ω_0 , (ii) the tunneling amplitude should be relatively small, not significantly larger than the bottom of the phonon dispersion, and (iii) there should be a large dielectric constant to reduce the destructive effect of long-range Coulomb interaction. With a possible compact and light bipolaron at the strong coupling limit with dispersive phonons, there will be more possibilities in the search for new materials with high superconducting temperatures.

ACKNOWLEDGMENTS

C.Z. thanks Nikolay Prokof'ev and Boris Svistunov for helpful discussions. This work is supported by the National Natural Science Foundation of China (NSFC) under Grants No. 12204173 and No. 12275263), the Innovation Program for Quantum Science and Technology (under Grant No. 2021ZD0301900), and the National Key R & D Program of China (under Grant No. 2018YFA0306501).

- [1] L. D. Landau, *Phys. Z. Sowjetunion* **3**, 664 (1933).
- [2] H. Fröhlich, H. Pelzer, and S. Zienau, *Philos. Mag.* **41**, 221 (1950).
- [3] R. P. Feynman, *Phys. Rev.* **97**, 660 (1955).
- [4] T. D. Schultz, *Phys. Rev.* **116**, 526 (1959).
- [5] T. Holstein, *Ann. Phys. (Amsterdam)* **8**, 325 (1959).
- [6] A. S. Alexandrov and P. E. Kornilovitch, *Phys. Rev. Lett.* **82**, 807 (1999).
- [7] T. Holstein, *Ann. Phys. (Amsterdam)* **281**, 725 (2000).

- [8] W. F. Brinkman and T. M. Rice, *Phys. Rev. B* **2**, 1324 (1970).
- [9] E. L. Nagaev, *Phys. Status Solidi B* **65**, 11 (1974).
- [10] N. F. Mott, *Adv. Phys.* **39**, 55 (2006).
- [11] A. Bulgac and M. M. Forbes, *Phys. Rev. A* **75**, 031605(R) (2007).
- [12] C. Lobo, A. Recati, S. Giorgini, and S. Stringari, *Phys. Rev. Lett.* **97**, 200403 (2006).
- [13] N. V. Prokof'ev and B. V. Svistunov, *Phys. Rev. B* **77**, 125101 (2008).

- [14] N. Prokof'ev and B. Svistunov, *Phys. Rev. B* **77**, 020408(R) (2008).
- [15] M. Kutschera and W. Wójcik, *Phys. Rev. C* **47**, 1077 (1993).
- [16] P. E. Kornilovitch and E. R. Pike, *Phys. Rev. B* **55**, R8634(R) (1997); **69**, 059902(E) (2004).
- [17] D. J. J. Marchand, G. De Filippis, V. Cataudella, M. Berciu, N. Nagaosa, N. V. Prokof'ev, A. S. Mishchenko, and P. C. E. Stamp, *Phys. Rev. Lett.* **105**, 266605 (2010).
- [18] J. Bonča, T. Katrasčnik, and S. A. Trugman, *Phys. Rev. Lett.* **84**, 3153 (2000).
- [19] A. Macridin, G. A. Sawatzky, and M. Jarrell, *Phys. Rev. B* **69**, 245111 (2004).
- [20] M. Capone, W. Stephan, and M. Grilli, *Phys. Rev. B* **56**, 4484 (1997).
- [21] C. A. Perroni, E. Piegari, M. Capone, and V. Cataudella, *Phys. Rev. B* **69**, 174301 (2004).
- [22] C. Zhang, N. V. Prokof'ev, and B. V. Svistunov, *Phys. Rev. B* **104**, 035143 (2021).
- [23] M. R. Carbone, A. J. Millis, D. R. Reichman, and J. Sous, *Phys. Rev. B* **104**, L140307 (2021).
- [24] C. Zhang, J. Sous, D. R. Reichman, M. Berciu, A. J. Millis, N. V. Prokof'ev, and B. V. Svistunov, *Phys. Rev. X* **13**, 011010 (2023).
- [25] J. Sous, C. Zhang, M. Berciu, D. Reichman, B. Svistunov, N. Prokof'ev, and A. Millis, [arXiv:2210.14236](https://arxiv.org/abs/2210.14236).
- [26] D. Jansen, J. Bonča, and F. Heidrich-Meisner, *Phys. Rev. B* **106**, 155129 (2022).
- [27] J. Bonča and S. A. Trugman, *Phys. Rev. B* **106**, 174303 (2022).
- [28] D. J. J. Marchand and M. Berciu, *Phys. Rev. B* **88**, 060301(R) (2013).
- [29] J. Bonča and S. A. Trugman, *Phys. Rev. B* **103**, 054304 (2021).
- [30] N. C. Costa, T. Blommel, W.-T. Chiu, G. Batrouni, and R. T. Scalettar, *Phys. Rev. Lett.* **120**, 187003 (2018).
- [31] C. Zhang, N. V. Prokof'ev, and B. V. Svistunov, *Phys. Rev. B* **105**, L020501 (2022).
- [32] W. P. Su, J. R. Schrieffer, and A. J. Heeger, *Phys. Rev. Lett.* **42**, 1698 (1979).
- [33] S. Barišić, J. Labbé, and J. Friedel, *Phys. Rev. Lett.* **25**, 919 (1970).
- [34] S. Barišić, *Phys. Rev. B* **5**, 932 (1972).
- [35] S. Barišić, *Phys. Rev. B* **5**, 941 (1972).